

# A Cold Low Noise Preamplifier for Use in Liquid Xenon

A. Pullia, F. Zocca, C. Olsen, P. Shagin, U. Oberlack

**Abstract**—In this paper a low-noise preamplifier for liquid-xenon ionization detectors is presented. The preamplifier has a cold front-end to be operated in liquid xenon at  $\sim 160$  K and a warm part installed 15-cm apart and working at room temperature. It features an unusually high sensitivity of  $\sim 70$  mV/fC. This specification is required because the net charge delivered in liquid xenon per unit energy is one order of magnitude lower than in silicon or germanium detectors. The preamplifier consists of a JFET-input charge-sensing stage with a feedback capacitance as low as 0.2 pF and a low-noise gain stage with differential output stage, able to drive  $50\Omega$  terminated cables. With a detector capacitance of 33 pF the preamplifier features an Equivalent Noise Charge of  $\sim 110$  electrons r.m.s. at a shaping time of 6  $\mu$ s, and a risetime of  $\sim 75$  ns.

## I. INTRODUCTION

In the context of R&D for a Liquid Xenon Time Projection Chamber (LXeTPC) as a Compton telescope for MeV gamma-rays, we have developed a low noise preamplifier with cold front-end inside liquid xenon. The LXeTPC approach shown in Fig. 1 exploits the excellent scintillation and ionization properties of ultrapure liquid xenon, in a temperature range of about 165-180K [1-2]. With a pair-creation energy of 15.6 eV, LXe is an efficient ionization medium and provides more charge than other noble liquids. Yet, the charge signals of  $\sim 1$  fC/100 keV are also significantly smaller than in semiconductor detectors. Operation as a Compton telescope requires both excellent energy resolution and low thresholds. Since the LXeTPC uses a cryogenic liquid as detector medium, it is usually made of a detector vessel and a cryostat. As a result, any measured charge signals must pass feed-throughs and typically substantial cable length before reaching a charge-sensitive amplifier (CSA). Placing a first amplification stage inside the xenon liquid has several potential benefits: it places the amplification stage in immediate proximity to the sensing electrodes, removing the input capacitance of long leads, and reducing the potential for noise pick-up. Furthermore, the operating temperature of the LXeTPC is near the noise optimum for Si-based electronics, hence reducing thermal noise in the preamplification without otherwise impeding the

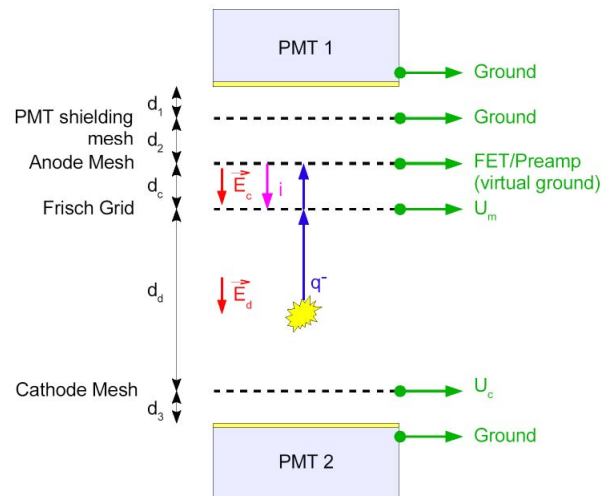


Fig. 1. Scheme of a LXeTPC detector. The ionization charge drifts through liquid xenon towards the anode, passing by a Frisch grid. The photomultipliers PMT 1 and PMT 2 on top and bottom are used to detect xenon scintillation light.

device performance. On the other hand, the location inside an LXeTPC also imposes significant constraints on this first amplification stage: insertion of electronegative impurities into the xenon liquid must not exceed the ppb level; the electronics and connections must withstand thermal cycling from a mild “baking” temperature of  $\sim 400$  K under vacuum to the low operating temperature inside LXe; and the introduction of excess heat must be reduced to a minimum, in order to avoid local formation of gas bubbles and to reduce heat load in general.

We present an approach that places the first-stage Junction Field Effect Transistor (JFET, Philips BF862) of an ultra-low noise charge sensitive amplifier on a board next to the sensing electrode inside LXe, together with the surface-mount resistor and capacitor feedback elements, as well as a capacitor for charge calibration with a testpulse. As shown in Fig. 2 this “cold stage” is connected with the remainder of the CSA through twisted pair cables: one pair each for feed-back, source/drain of the JFET, and the testpulse input. The main CSA stage is placed in a box directly connected to a detector feed-through. The Milan group developed a custom CSA to match the requirements of the LXe detector. In particular, the

A. Pullia and F. Zocca are with the University of Milan, Department of Physics and Istituto Nazionale di Fisica Nucleare, Milano, Italy.

U. Oberlack, C. Olsen, and P. Shagin are with the Dept. of Physics & Astronomy, Rice University, Houston, TX, USA.

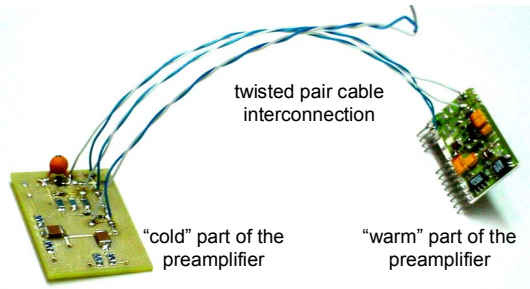


Fig. 2. Photograph of the “cold” and “warm” parts of the preamplifier, as linked by twisted pair cables.

gain was brought to a level of  $\sim 70$  mV/fC into a differential (100  $\Omega$ ) output, to match the  $\pm 1$  V differential input range of an FADC board sampling the signal. The Rice group designed the cold stage.

In this paper we discuss the preamplifier circuit structure and performance. A complete testbench characterization is presented. The integration of this system in the Rice *XeSpec* detector is in progress and will be discussed elsewhere.

## II. PREAMPLIFIER STRUCTURE

In Fig. 3 the schematic diagram of the realized circuit is shown, and the components on the “cold” and “warm” boards are put into evidence. It basically consists of a negative-feedback charge-sensing stage, using  $C_F$ ,  $R_{F1}$ ,  $R_{F2}$ ,  $R_{F3}$ , as feedback network, followed by a single-ended to differential gain-stage built around operational amplifiers  $U_1$  and  $U_2$ , configured as an “instrumentation amplifier”. The charge

sensing stage is in practice an active integrator with a continuous reset time-constant given by  $\tau_F = C_F \times (R_{F1} + R_{F2} + R_{F3})$ , or 600  $\mu$ s nominally. The forward path of the integrator has a simple folded-cascode structure ( $Q_1$  and  $Q_2$ ) with an active load ( $Q_3$ ).

Input “HV” provides low-pass filtering for the detector high-voltage bias by means of  $R_{H2}$  and  $C_H$ . Input “DETECTOR” is therefore biased to the high voltage provided by “HV”. The detector signal current entering pin “DETECTOR” is AC coupled to the preamplifier and reaches the preamplifier’s input, or the JFET’s gate, through CR network  $C_B$ ,  $R_{H1}$ . Input “TEST” is used to inject a detector-like calibration testpulse to the preamplifier’s input pin.

The response of the circuit to a detector charge signal  $Q$  is in first approximation a step function with amplitude

$$V_{OUT} = -Q \times \frac{1}{C_F} \left( 1 + \frac{R_8}{R_9} \right), \quad (1)$$

$$V_{IOUT} = Q \times \frac{1}{C_F} \frac{R_{10}}{R_9}. \quad (2)$$

Note that as the detector electrode collects negative charge  $V_{OUT}$  is positive and  $V_{IOUT}$  is negative. In a better approximation the step shows a slow exponential decay with time constant  $\tau_F$  due to the continuous-time discharge of  $C_F$  through the series of resistors  $R_{F1}$ ,  $R_{F2}$ , and  $R_{F3}$ . The reason why a series of three resistors was used rather than an individual one will be discussed in the next section. The preamplifier overall sensitivity is derived from (1) and (2), or

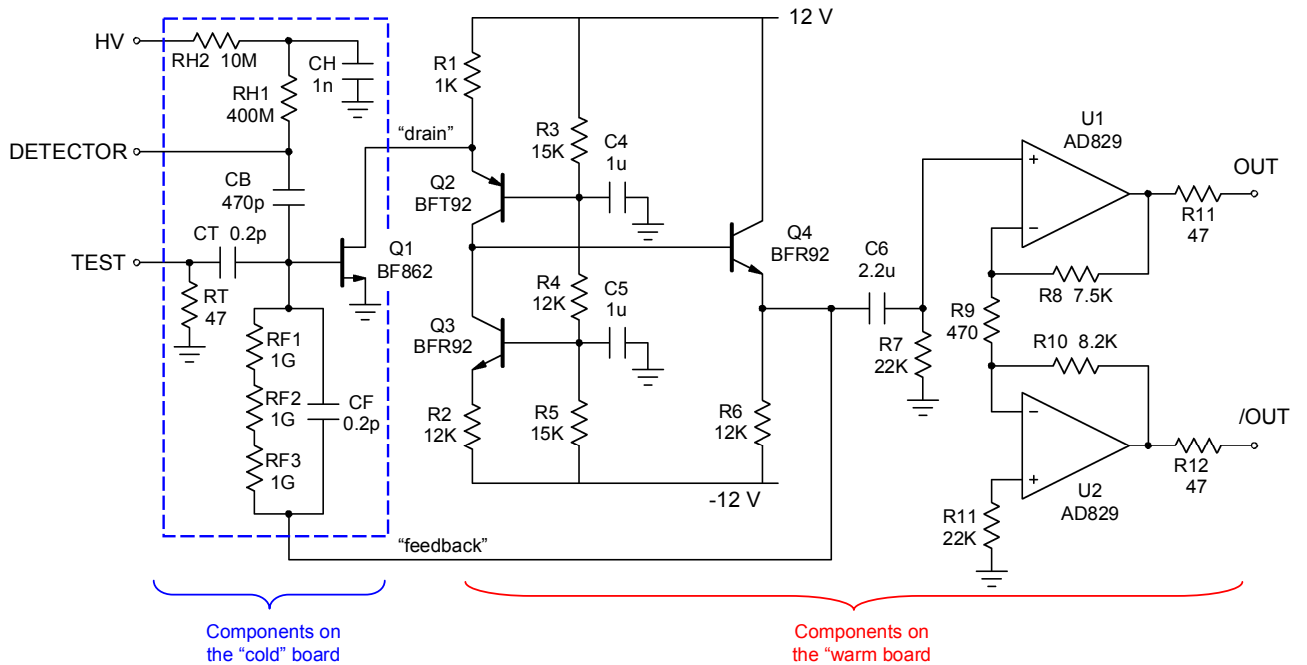


Fig. 3. Simplified schematic diagram of the charge sensitive preamplifier.

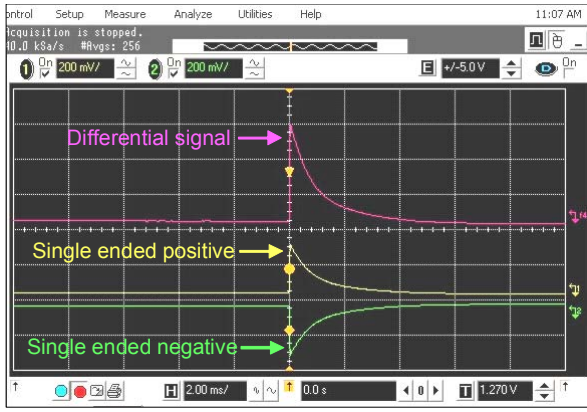


Fig. 4. Oscilloscope screenshot showing the preamplifier response to a test signal in the ms time scale. X-axis: 2ms/div, Y-axis: 200mV/div. A 50 $\Omega$  load is present on both oscilloscope channels. The DC offset of the differential signal is <50mV. The exponential-decay time constant is of  $\sim 800 \mu\text{s}$ .

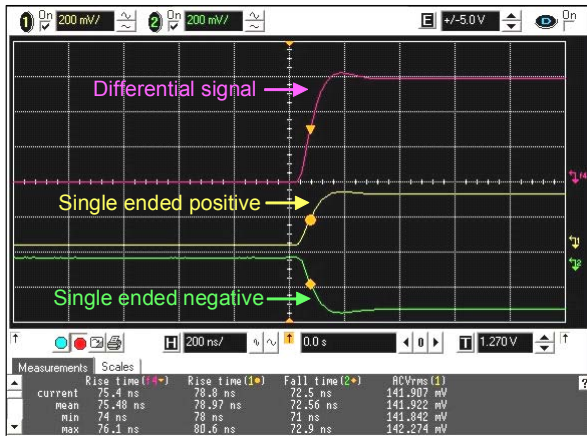


Fig. 5. Oscilloscope screenshot showing the preamplifier response to a test signal in the  $\mu\text{s}$  time scale. X-axis: 200ns/div, Y-axis: 200mV/div. A 50 $\Omega$  load is present on both oscilloscope channels. A risetime of  $\sim 75 \text{ ns}$  is obtained on the differential signal.

$$\left| \frac{V_{OUT} - V_{IOUT}}{Q} \right| = \frac{1}{C_F} \left( 1 + \frac{R_8}{R_9} + \frac{R_{10}}{R_9} \right) \quad (3)$$

If the differential output signal is transmitted to a remote FADC through a terminated cable, the sensitivity (3) becomes

$$\left| \frac{\Delta V_{FADC}}{Q} \right| = \frac{1}{C_F} \left( 1 + \frac{R_8}{R_9} + \frac{R_{10}}{R_9} \right) \frac{1}{2} \quad (4)$$

as the signal gets splitted by half across the termination resistors.

In order to implement the large required sensitivity of  $\sim 70 \text{ mV/fC}$  a low-value feedback capacitance  $C_F$  of 0.2 pF has been used, and a relatively large gain of  $\sim 17$  has been

TABLE I  
RELEVANT PARAMETERS OF AD829

Input voltage noise @ 1 kHz	Input current noise @ 1 kHz	Bandwidth of inverting or non inverting amplifiers (1k $\Omega$ load)	Output swing into a 150 $\Omega$ load
1.7 nV/ $\sqrt{\text{Hz}}$	1.5 pA/ $\sqrt{\text{Hz}}$	65 MHz @ G=-9 or G=+10	$\pm 3 \text{ V}$
		55 MHz @ G=-19 or G=+20	
		39 MHz @ G=-24 or G=+25	

implemented in each branch of the differential output stage. We used the AD829 opamps in the differential output stage because it has an extremely low noise, a large output voltage swing, and a relatively large bandwidth even at high gains. Table I shows some relevant parameters of the AD829. Note that the effective value of  $C_F$  including the stray components, is expected to be in the 2.5 to 3 pF range.

The so-obtained high sensitivity poses a few design issues, some of which are evident while some others are more subtle, as shown in the following section.

### III. DESIGN ISSUES AND EXPERIMENTAL RESULTS

A first issue related to the high circuit gain is the potential high DC offset at the preamplifier output, enhanced by the presence of a negative DC bias voltage at the input JFET's gate. As shown in Fig. 3 we addressed this issue by AC coupling the output stage by means of  $C_6$ ,  $R_7$  and by using resistor  $R_{11}$  for compensating the bias currents of the Analog Devices AD829 operational amplifiers. We so obtained a DC offset for the differential signal  $V_{OUT} - V_{IOUT}$  of the order of -50 mV, as shown in Fig. 4. Fig. 4 also shows the exponential-decay transient with an observed time constant of  $\sim 800 \mu\text{s}$ . Fig. 5 is a blow up of Fig. 4 in the microsecond time scale showing the  $\sim 75 \text{ ns}$  rise time of the preamplifier, which is to be regarded as a good performance when using a detector capacitance as large as 33 pF, a feedback capacitance as low as of 0.2 pF and while driving terminated 50  $\Omega$  output cables. Such a rise time is in any event adequate for this application.

A second more subtle issue related to the high circuit gain is its extreme sensitivity to any voltage ringing directly or indirectly coupled to a few preamplifier's sensitive points in the charge sensing stage. In particular the circuit shows a tendency to pick up any ringing of the positive power-supply and of a few imperfect ground points. Even if the power supply is strongly filtered it inevitably rings slightly when the output signal swiftly rises. The ringing becomes apparent when the preamplifier outputs are connected to terminated cables, i.e. to low-value equivalent resistances, and so a remarkable current has to flow from the power supply to ground in a short while. In our case the power-supply ringing is mostly picked up through resistance  $R_1$ , and the ground ringing is mostly picked up by capacitance  $C_4$ . As a result the output waveform appeared distorted when using the terminated cables. The distortion disappeared by disconnecting the terminated cables. We could greatly reduce this undesired effect by: (a) using separate filters for the +12V power supply used in the charge

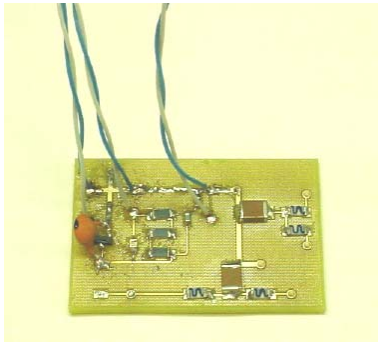


Fig. 6. Photograph of the “cold” preamplifier board. The feedback resistor can be seen in the center-left region of the board as realized as the series of three chip resistors.

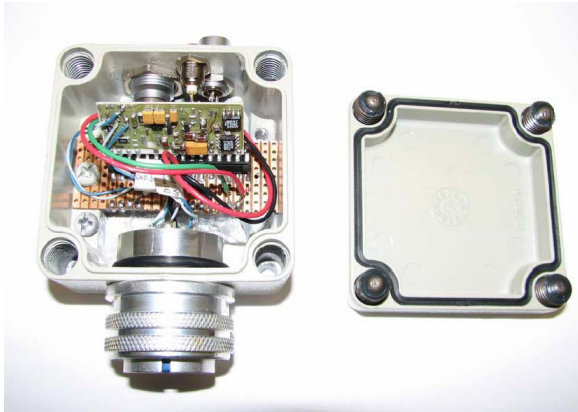


Fig. 7. Photograph of the “warm” part of the preamplifier as mounted in its hermetic shielded box. The two twisted pair cables used to connect the “warm” to the “cold” part pass through the big cylindrical connector.

sensing stage and that used for the operational amplifiers, and (b) re-laying out the ground via of  $C_4$  in such a way to separate it physically as much as possible from the ground vias used for the opamps power-supply filters.

Special care has also been devoted to the connection between the “cold” and “warm” preamplifier boards. As shown in Fig. 3 such connection consists basically of the “drain” and the “feedback” wires plus an implicit ground link. Each of these links was realized with a twisted pair cable. The two wires of the first pair are “drain” and “ground”, the two wires of the second pair are “feedback” and “ground”. The “ground” wires provide an easy path for the high-frequency return currents, which greatly helps stabilize the feedback and reduce the Electro Magnetic Interferences (EMI) [3].

We are now to discuss a few other issues concerning the cold preamplifier board.

As can be seen in Fig. 3 and Fig. 6 the feedback resistor is realized in practice as the series of three  $1\text{ G}\Omega$  resistors. This approach yields a reduced intrinsic stray capacitance. In fact the stray capacitance of a chip resistor depends mostly on its geometry and is of the order of  $150\text{ fF}$  for the 0805 size. Use of three resistors in series makes the intrinsic stray capacitance three times as low, i.e. of the order of  $50\text{ fF}$ . Minimization of

all stray capacitances is evidently important in our circuit, which needs a feedback capacitance as low as  $0.2\text{ pF}$  to implement a high charge sensitivity.

Finally, we carefully studied and optimized the grounding of the “cold” preamplifier board. On the one hand a ground plane under the JFET and feedback devices greatly helps reduce the low-frequency disturbances, or microphonism, as it works as an electro-magnetic shield against all stray capacitances which could enhance and modulate the effective feedback capacitance value. For example the stray capacitance between the two traces/pins used for the feedback capacitor depends in part on the physical distance of the “cold” preamplifier board from the grounded mechanical parts in immediate proximity, and is sensitive to any mechanical vibrations. It should therefore be shielded. On the other hand a ground plane under the three feedback resistors  $R_1$ ,  $R_2$  and  $R_3$  creates two new capacitive paths from the intermediate connection points between these resistors to ground. These stray capacitances yield an apparent distortion of the exponential-decay shape of the preamplifier response, as can be shown analytically and experimentally. So, we found that the optimal solution consists of laying out a ground plane under all input/feedback devices but the feedback resistors.

#### IV. NOISE MEASUREMENTS

We eventually installed the “warm” part of the preamplifier in the hermetic shielded box shown in Fig. 7. We used a capacitance of  $33\text{ pF}$  to simulate the detector and arranged the “cold” part of the preamplifier with or without a ground plane underneath. In these testbench measurements the “cold” preamplifier could not be cooled to cryogenic temperatures, and was operated at room temperature. For signal-to-noise optimization we used a Gaussian shaper, Ortec 572, with selectable shaping time in the  $0.5$  to  $10\text{ }\mu\text{s}$  range. In the first tests we used  $13\text{-cm}$  long twisted pair cables to connect the “cold” and “warm” parts of the preamplifier and housed both parts in the same shielded box. The “cold” board had no ground plane underneath. The CSA showed a sensitivity of  $\sim 62\text{ mV/fC}$  and an excellent noise performance with a minimum of  $\sim 110$  electrons achieved for a shaping time of  $6\text{ }\mu\text{s}$ , as shown in Fig. 8, which is adequate for the foreseen applications. Cooling of the cold part of the preamplifier will help reduce the noise further. No significant difference in the noise performance was observed using a grounded “cold” preamplifier board. However as expected the presence of a ground plane definitely made the system less sensitive to microphonism. In Fig. 8 the ENC values have been fitted and the principal noise contributions have been disentangled using the procedure described in [4,5]. The dominant contribution to the ENC in the  $2$  to  $10\text{ }\mu\text{s}$  shaping-time range is the flat one, due to the  $1/f$  noise of the JFET and the dielectric noise of the FR4 board where the JFET is mounted [6]. This noise contribution could be reduced using a higher quality dielectric, like teflon or alumina [7]. Cryogenic cooling will also help reduce this noise component.

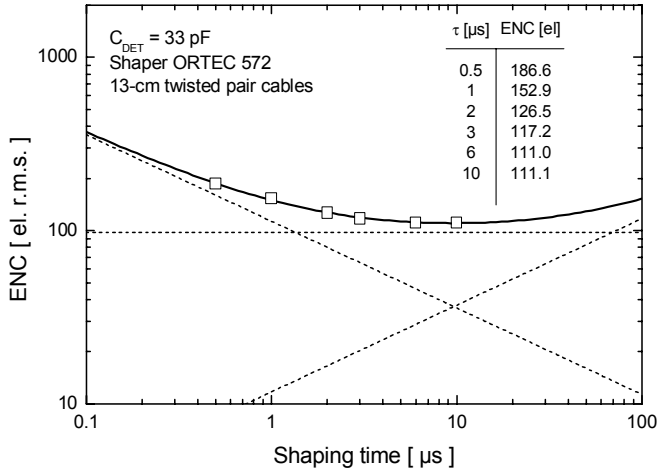


Fig. 8. ENC vs. shaping time as measured placing the “cold” and “warm” parts of the preamplifier in the same shielded box, and using a “cold” preamplifier board with no ground plane.

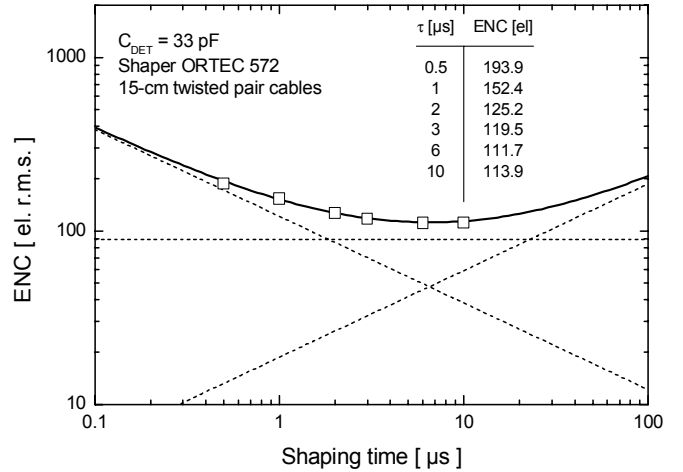


Fig. 9. ENC vs. shaping time as measured using a “cold” preamplifier board with a ground plane underneath.

We eventually placed the grounded “cold” part of the preamplifier in a separated box using the hermetic feed-through shown in Fig. 7. In this case the overall length of the connection between the “cold” and “warm” parts of the preamplifier was 15 cm. The CSA showed a sensitivity of  $\sim 75$  mV/fC and again an excellent noise performance with a minimum of  $\sim 110$  electrons achieved for a shaping time of 6  $\mu$ s, as shown in Fig. 9. As can be seen in this case the charge sensitivity is higher and the noise is just a little bit higher. The increase in the charge sensitivity depends on the shielding effect of the ground plane, which remarkably reduces the stray capacitance between the feedback capacitance traces. The little noise increase could depend on the absence of an effective shielding along the connection between the “cold” and “warm” parts. Also in this case the dominant noise contribution is related to the  $1/f$  noise of the JFET and to the dielectric noise of the FR4 board where the JFET is installed.

## V. CONCLUSION

We designed, realized, and testbench characterized a low-noise preamplifier for use in Liquid Xenon Time Projection Chamber for MeV gamma-rays detection. The Charge Sensitive Amplifier showed a high sensitivity of  $\sim 75$  mV/fC, a risetime of  $\sim 75$  ns and an excellent noise performance with a minimum of  $\sim 110$  electrons achieved for a shaping time of 6  $\mu$ s. Work is in progress to integrate this electronic system in the Rice *XeSpec* detector.

## VI. ACKNOWLEDGEMENTS

The authors acknowledge R. Bassini and C. Boiano for technical assistance. This work was supported in part under NASA grant NNG05WC24G.

## VII. REFERENCES

- [1] E. Aprile, A. Curioni, V. Egorov, K.L. Giboni, U. Oberlack, S. Ventura, T. Doke, K. Takizawa, E.L. Chupp, P.P. Dunphy, “A Liquid Xenon Time Projection Chamber for Gamma-Ray Imaging in Astrophysics: Present Status and Future Directions”, *Nucl. Instr. Meth.*, vol. A461, pp. 256–261, 2001.
- [2] U. Oberlack, E. Aprile, “A Study of Liquid Xenon Detectors with Enhanced Spectroscopy and Time-of-Flight Background Rejection for an Advanced Compton Telescope”, NASA proposal APRA04-0084-0051, 2004. URL: <http://astroparticlelab.rice.edu/>
- [3] See e.g. H. W. Ott, “Noise Reduction Techniques in Electronic Systems”, Wiley and Sons, p. 140, New York, 1976.
- [4] G. Bertuccio and A. Pullia, “A Method for the Determination of the Noise Parameters in Preamplifying Systems for Semiconductor Radiation Detectors”, *Rev. Sci. Instr.*, vol. 64, no. 11, pp. 3294-3298, 1993.
- [5] E. Gatti, P.F. Manfredi, M. Sampietro, V. Speziali, “Suboptimal filtering of  $1/f$  noise in detector charge measurements”, *Nucl. Instr. Meth.*, vol. A297, pp. 467-478, 1990.
- [6] V. Radeka, “Field Effect Transistors for Charge Amplifiers”, *IEEE Trans. Nucl. Sci.*, vol. NS-20, no. 1, pp. 182-189, 1973.
- [7] A. Pullia, G. Bertuccio, “Resolution limits of silicon detectors and electronics for soft X-ray spectroscopy at non cryogenic temperatures”, *Nucl. Instrum. and Meth.*, vol. A380, pp. 1-5, 1996.